

# Multi-task Gaze Estimation Via Unidirectional Convolution

Zhang Cheng

College of Computer and Information Science  
Chongqing Normal University  
Chongqing, China  
2022210516040@stu.cqnu.edu.cn

Yanxia Wang\*

College of Computer and Information Science  
Chongqing Normal University  
Chongqing, China  
wangyanxia@cqnu.edu.cn

**Abstract**—Using lightweight models as backbone networks in gaze estimation tasks often results in significant performance degradation. The main reason is that the number of feature channels in lightweight networks is usually small, which makes the model expression ability limited. In order to improve the performance of lightweight models in gaze estimation tasks, a network model named Multitask-Gaze is proposed. The main components of Multitask-Gaze include Unidirectional Convolution (UC), Spatial and Channel Attention (SCA), Global Convolution Module (GCM), and Multi-task Regression Module (MRM). UC not only significantly reduces the number of parameters and FLOPs, but also extends the receptive field and improves the long-distance modeling capability of the model, thereby improving the model performance. SCA highlights gaze-related features and suppresses gaze-irrelevant features. The GCM replaces the pooling layer and avoids the performance degradation due to information loss. MRM improves the accuracy of individual tasks and strengthens the connections between tasks for overall performance improvement. The experimental results show that compared with the State-of-the-art method SUGE, the performance of Multitask-Gaze on MPIIFaceGaze and Gaze360 datasets is improved by 1.71% and 2.75%, respectively, while the number of parameters and FLOPs are significantly reduced by 75.5% and 86.88%.

**Index Terms**—Multitask, lightweight, gaze estimation, Unidirectional Convolution, Spatial and Channel Attention.

## I. INTRODUCTION

Gaze estimation reveals human intention information and points of interest, and is widely used in various fields such as autonomous driving [1], human-computer interaction [2], psychological research [3], and medical diagnosis [4] [5]. The gaze estimation methods can be divided into two types: model-based [6] [7] and appearance-based [8] [9]. Model-based methods rely on eye structure models and can achieve high accuracy, but this method requires specialized equipment and has limited usage scenarios. The appearance-based method is less restricted by the environment and has a simple device, and deep learning techniques can be used to predict gaze direction from direct facial or eye images. In recent years, appearance-based methods have gradually become a research hotspot due to their convenience and wide application scenarios.

However, current appearance-based methods mostly improve model performance by increasing network depth, while

performance degrades when performing gaze estimation tasks using lightweight networks. In order to improve the above problems, a variety of lightweight networks such as FR-Net [10] and GazeNAS-ETH [11] have been proposed. However, FR-Net uses higher resolution images as input data, which increases the computational burden and reduces the real-time performance of the model. GazeNAS-ETH requires parameter search of the model on a large dataset to achieve advanced performance. Lightweight models have a wider range of application scenarios, but are also more challenging because it is difficult to balance the number of model parameters and accuracy. Therefore, lightweight model still has important research significance.

An important reason for the performance degradation of lightweight models is that the number of feature channels is small, which leads to the lack of fitting ability. In addition, lightweight models usually use deep convolution [12] instead of standard convolution, because the lack of inter-channel information fusion in deep convolution reduces the model's expressiveness. One possible solution is to fuse attention mechanism in the network, make it pay more attention to gaze-related information.

In this paper, we propose a lightweight multi-task gaze estimation model for the above problem. This model not only further reduces the parameters of the existing lightweight model, but also better balances the number of parameters and performance of the model.

The main contributions of this paper are as follows:

- A Unidirectional Convolution (UC) is proposed. UC replaces deep convolution, which not only significantly reduces the number of parameters and FLOPs, but also extends the receptive field of the model to improve the long-distance modeling capability and hence the model performance.
- A new Spatial and Channel Attention (SCA) is proposed. spatial attention realizes global information perception at the spatial level, making full use of context information and increasing the weight of important information in space. channel attention realizes information interaction between channels.
- A Global Convolutional Module (GCM) based on UC is proposed. GCM replaces the pooling layer to fur-

\* is corresponding author.

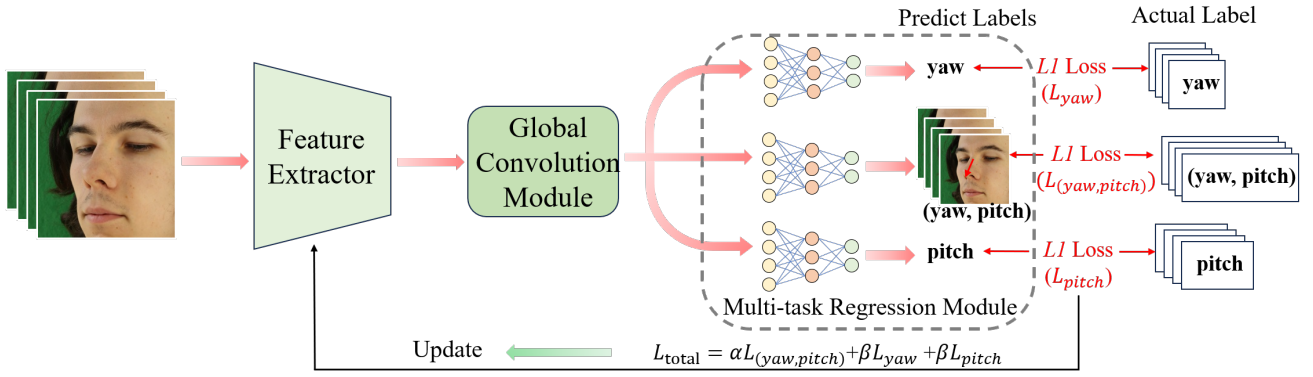


Fig. 1. Structure of Multitask-Gaze

ther integrate global information and avoid performance degradation caused by information loss.

- A Multi-task Regression Module (MRM) is proposed. The model improves the performance of individual tasks and strengthens the correlation between tasks, thereby improving the overall performance.

## II. METHODS

This section details the proposed Multitask-Gaze network model, which consists of three components: Feature Extractor, Global Convolution Module, and Multi-task Regression Module. The structure is shown in Fig. 1.

### A. Feature Extractor

The feature extractor is improved based on MobileNetV3 [13], and the main difference from the original MobileNetV3 is the use of UC to improve the neck block, while adding SCA after the 3rd, 6th, and 9th neck blocks, respectively.

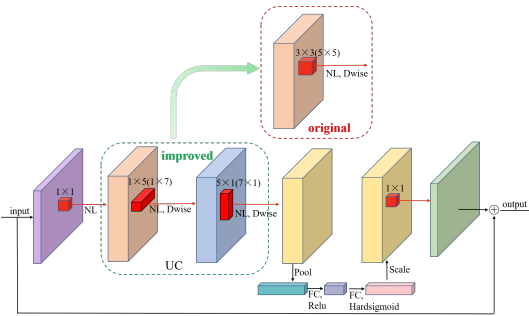


Fig. 2. Structure of neck

**Unidirectional Convolution(UC).** Neck is the basic building block of a network, and its structure is shown in Fig. 2. In this paper, we improve the neck module with UC to make it more lightweight. In order to expand the receptive field of the model and fully integrate contextual information to improve performance, this paper replaces the  $3 \times 3$  or  $5 \times 5$  convolutions in the original neck structure with UC of  $[1 \times 5; 5 \times 1]$  or  $[1 \times 7; 7 \times 1]$ , respectively. Assuming the size of the output feature map is  $H_{out} * W_{out}$ , the convolution kernel is  $K_H * K_W$ , the input

channel is  $C_{in}$ , and the output channel is  $C_{out}$ , the parameter and computational complexity of the improved part in neck are as follows:

$$\begin{aligned}
 Para_{original} &= K_H * K_W * C_{in} * C_{out} \\
 Para_{UC} &= 1 * K_W * C_{in} * C_{out} + K_H * 1 * C_{in} * C_{out} \\
 FLOPs_{original} &= (K_H * K_W * C_{in} * C_{out}) * H_{out} * W_{out} \\
 FLOPs_{UC} &= (1 * K_W * C_{in} * C_{out}) * H_{out} * W_{out} \\
 &\quad + (K_H * 1 * C_{in} * C_{out}) * H_{out} * W_{out}
 \end{aligned} \tag{1}$$

When both the input and output channels are 40, the output feature map size is  $56 \times 56$ , and the original convolution kernel is  $5 \times 5$ , UC reduces the number of parameters and FLOPs by at least 44%.

**Spatial and Channel Attention(SCA).** In lightweight networks, standard convolutions are usually replaced with deep convolutions to achieve lightweighting, but there is no information exchange between deep convolution channels, resulting in performance degradation. In order to compensate for the shortcomings of deep convolution, SCA is proposed in this paper, whose structure is shown in Fig. 3. SCA is divided into two parts: Spatial Attention and Channel Attention. Spatial Attention not only highlights important features at the spatial level, but also achieves global spatial information exchange through the shift window mechanism [14], enhancing the model's long-distance modeling capability. The Channel Attention further integrates global information through average pooling, extracts the most significant features through max-pooling, and then uses MLP to complete information exchange between channels.

### B. Global Convolution Module

In CNN, when classifying or regressing various tasks, it is usually necessary to first perform global information fusion on the feature maps through global average pooling. However, global average pooling will to some extent ignore local details and differences in the feature map, and if important information is lost, it will lead to performance degradation. On the other hand, if there are outliers in the feature map, they may have a significant impact on the results of global

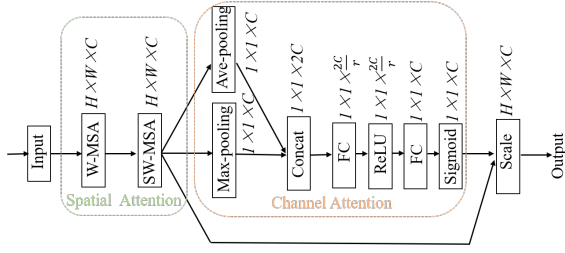


Fig. 3. Structure of SCA

average pooling, thereby reducing the robustness and accuracy of the model. In terms of the above issues, this paper proposes a Global Convolution Module (GCM) based on UC, which integrates global information without causing information loss. Its structure is shown in Fig. 4.

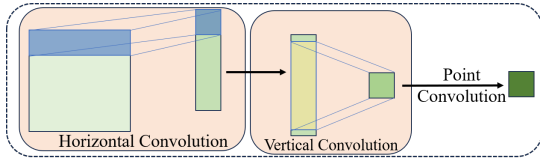


Fig. 4. Structure of GCM

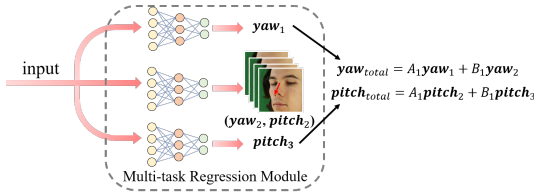


Fig. 5. Structure of MRM

### C. Multi-task Regression Module

The function of the Multi-task Regression Module (MRM) is to predict yaw, (yaw, pitch) and pitch respectively, by using the feature  $f \in \mathbb{R}^{1 \times 1 \times 480}$  extracted by GCM. Its structure is shown in Fig. 5. The MRM consists of three MLP modules, with two MLP modules predicting yaw and pitch, respectively, to improve the accuracy of a single Angle. However, human gaze change is usually a process of continuous change, there is a certain correlation between yaw and pitch, and individual prediction may not be able to make full use of the intrinsic connection and interdependence between yaw and pitch, thus limiting the comprehensive performance. To solve this problem, this paper adds another MLP module to predict yaw and pitch at the same time, and finally assigns different weight parameters to yaw and pitch through hyperparameter setting. The calculation formula is as follows:

$$\begin{aligned}
 (yaw_1, pitch_1) &= (MLP_1(f), MLP_3(f)) \\
 (yaw_2, pitch_2) &= MLP_2(f) \\
 yaw_{total} &= A_1 yaw_1 + B_1 yaw_2 \\
 pitch_{total} &= A_1 pitch_1 + B_1 pitch_2
 \end{aligned} \tag{2}$$

TABLE I  
COMPARISON WITH STATE-OF-THE-ART METHODS.

| Methods             | Params(M) | FLOPs(G) | G [16] | MPII [17] | RT [18] | Year |
|---------------------|-----------|----------|--------|-----------|---------|------|
| Dilated-Net [20]    | 3.92      | 3.15     | 13.73° | 4.42°     | 8.38°   | 2018 |
| Gaze360 [16]        | 11.90     | 7.29     | 11.04° | 4.06°     | 7.06°   | 2019 |
| GazeTR [21]         | 11.42     | 1.83     | 10.62° | 4.00°     | 6.55°   | 2022 |
| CADSE [22]          | 74.80     | 19.75    | 10.70° | 4.04°     | 7.00°   | 2022 |
| L2CS-Net [23]       | 23.52     | 16.53    | 10.41° | 3.92°     | N/A     | 2023 |
| GazeCaps [24]       | 11.70     | 1.82     | 10.04° | 4.06°     | 6.92°   | 2023 |
| Gaze-Swin [25]      | 32.28     | 5.17     | 10.14° | N/A       | 6.38°   | 2024 |
| SUGE [26]           | 11.42     | 1.83     | 10.51° | 4.01°     | N/A     | 2024 |
| MobileNetV3 [13]*   | 4.205     | 0.233    | 10.46  | 4.05      | 6.37    |      |
| Multitask-Gaze(Our) | 2.822     | 0.243    | 10.33° | 3.90°     | 6.35°   |      |

\* indicates performance applied to gaze estimation tasks, not original paper data

Where  $A_1 = B_1 = 0.5$ ,  $f$  represents the feature input to MRM.

## III. EXPERIMENTAL

### A. Implementation Details

In this paper, four datasets of ETH-XGaze [15], Gaze360 [16](G), MPIIFaceGaze [17](MPII), and RT-Genie [18](RT) were used to verify the performance of Multitask-Gaze model. ETH-Xgaze is used as the pre-training dataset. In order to effectively avoid overfitting of low-level features and loss of high-level semantics, a linear decay random dropout rate [19] is added to the three SCA modules during training. The parameter number, FLOPs, and Angle error (the smaller angular error indicates the better model performance) are used as evaluation metrics in this paper, and the Angle error is calculated as follows.

$$L_{angular} = \arccos\left(\frac{g \cdot \hat{g}}{\|g\| \|\hat{g}\|}\right) \tag{3}$$

Among them,  $g \in \mathbb{R}^3$  represents the actual gaze direction,  $\hat{g} \in \mathbb{R}^3$  represents the predicted gaze direction.

The loss function adopts MAE Loss (Mean Absolute Error), and the calculation formula is as follows:

$$\begin{aligned}
 (L_{yaw}, L_{pitch}) &= \left( \frac{1}{N} \sum_{i=1}^N |g_{yaw}^i - \hat{g}_{yaw}^i|, \frac{1}{N} \sum_{i=1}^N |g_{pitch}^i - \hat{g}_{pitch}^i| \right) \\
 L_{(yaw, pitch)} &= \frac{1}{N} \sum_{i=1}^N |g_{(yaw, pitch)}^i - \hat{g}_{(yaw, pitch)}^i| \\
 L_{total} &= A_2 L_{(yaw, pitch)} + B_2 L_{yaw} + B_2 L_{pitch}
 \end{aligned} \tag{4}$$

Where  $A_2 = 1, B_2 = 0.5$ ,  $N$  represents the number of samples.

### B. Comparison with State-of-the-art methods

This section compares Multitask-Gaze with existing state-of-the-art models in terms of angular error, parameters, and FLOPs, and the results are shown in Table 1. As can be seen from Table 1, although the Angle error of Gaze360 dataset by Gaze-Swin [25] is 0.19° (1.84%) lower than that of Multitask-Gaze, the parameter number and FLOPs of Multitask-Gaze are reduced by 91.2% and 95.36% respectively. Compared with the original MobileNetV3, Multitask-Gaze has a 0.13° (1.24%), 0.15 (3.7%) and 0.02 (0.3%) reduction in Angle errors on the Gaze360, MPIIFaceGaze and RT-Genie datasets, respectively. The parameters are further reduced by 32.9%, thus proving

TABLE II  
ABLATION EXPERIMENT

| Methods        | Params(M) | FLOPs(G) | G [16] | MPII [17] | RT [18] |
|----------------|-----------|----------|--------|-----------|---------|
| Multitask-Gaze | 2.828     | 0.243    | 10.33° | 3.90°     | 6.35°   |
| -MRM           | 2.735     | 0.243    | 10.62° | 3.88°     | 6.72°   |
| -SCA           | 2.743     | 0.204    | 10.86° | 3.86°     | 6.55°   |
| -GCM           | 2.816     | 0.250    | 10.73° | 3.88°     | 6.87°   |
| -ALL           | 2.639     | 0.211    | 11.01° | 3.84°     | 7.00°   |

- Indicate the removal of the corresponding model.

TABLE III  
VALIDATION OF GCM EFFECTIVENESS

| Methods     | G [16] | MPII [17] | RT [18] |
|-------------|--------|-----------|---------|
| GCM         | 10.33° | 3.90°     | 6.35°   |
| Avg-pooling | 10.73° | 3.88°     | 6.87°   |
| Max-pooling | 10.73° | 3.99°     | 6.77°   |

that Multitask-Gaze can further achieve lightweight while improving accuracy. The performance of Multitask-Gaze is improved for the following reasons:

- SCA uses an attention mechanism to highlight gaze-related information while enhancing spatial and channel information interactions.
- UC significantly expands the receptive field of the model and enhances long-distance modeling capabilities, utilizing a wider range of contextual information.
- GCM further fuses global information and reduces information loss.

### C. Ablation experiment

In order to better understand the effects of different modules on the Angle error, parameter number and FLOPs of the Multitask-Gaze model, the ablation experiment was performed in this section and the results were shown in Table 2. MRM has the largest relative impact on the number of model parameters, while SCA has the largest impact on FLOPs. In addition, the Angle error decreased after the corresponding module was removed from the MPIIFaceGaze dataset, which may have been slightly overfitting due to the small size of the dataset. However, for the other two datasets, there is a large performance degradation after the removal of the corresponding module. When all modules are removed, the performance on the RT-Genie dataset decreases significantly by 10.24%.

### D. Validation of GCM effectiveness

In order to verify whether GCM can improve the performance of the model, we experimentally replace GCM with global average pooling and max-pooling. The experimental results are shown in Table 3. After replacing GCM with Max-pooling, performance degradation occurred on each dataset. The reason for the performance degradation was that Max-pooling only selected the largest pixel in the feature map for backward propagation, resulting in severe information loss. When the feature map was  $5 \times 5$ , the information loss rate was as high as 96%, and Max-pooling lacked information interaction between channels.

TABLE IV  
VALIDATION OF UC EFFECTIVENESS

| Number of layers |           | Standard Convolution | UC         | UC         |
|------------------|-----------|----------------------|------------|------------|
|                  |           | 5x5                  | [5x1; 1x5] | [7x1; 1x7] |
| 3                | Params(M) | 0.04                 | 0.016      | 0.023      |
|                  | FLOPs(G)  | 0.083                | 0.05       | 0.07       |
| 4                | Params(M) | 0.08                 | 0.032      | 0.045      |
|                  | FLOPs(G)  | 0.087                | 0.052      | 0.072      |

### E. Validation of UC effectiveness

This section compares the parameter and FLOPs of UC and standard convolution, and visualizes the receptive field using the method proposed by Ding et al. [27]. The data are shown in Table 4 and Fig. 6. Based on Table 4 and Fig. 6, it can be seen that the receptive field size of the 3-layer  $5 \times 5$  standard convolution and the 3-layer  $[5 \times 1; 1 \times 5]$  UC are similar, but the UC has 60% fewer parameters and 39.76% fewer FLOPs than the standard convolution. However, the receptive field of the  $[7 \times 1; 1 \times 7]$  UC is significantly larger and the parameters and computational complexity are 42.5% and 15.66% less, respectively, than the standard convolution. The receptive fields of 4-layer  $5 \times 5$  standard convolution and 3-layer  $[7 \times 1; 1 \times 7]$  UC are roughly the same, but the parameters and computational complexity of 3-layer  $[7 \times 1; 1 \times 7]$  UC are significantly reduced by 71.25% and 19.54%, respectively. Therefore, larger UC can be used instead of smaller standard convolutions, which not only makes the model lighter, but also significantly expands the receptive field to capture a wider range of contextual information, thereby achieving performance improvement.

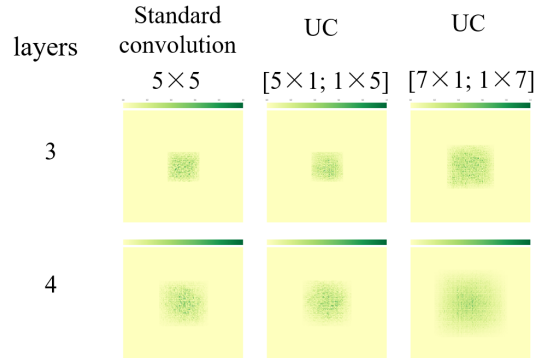


Fig. 6. Visualization of receptive field

## IV. CONCLUSION

In this paper, we propose a new lightweight model, Multitask-Gaze, and verify the model performance on a widely used dataset. The Multitask-Gaze is not only more lightweight, but also significantly improves performance. The advantages of the SCA, UC, GCM and MRM modules presented in this paper are strongly demonstrated, where SCA and GCM can achieve plug-and-play effects and provide new ideas for model lightweighting.

## REFERENCES

- [1] P. K. Sharma and P. Chakraborty, "A review of driver gaze estimation and application in gaze behavior understanding," *Engineering Applications of Artificial Intelligence*, vol. 133, p. 108117, 2024.
- [2] V. Somashekarappa, A. Sayeed, and C. Howes, "Neural network implementation of gaze-target prediction for human-robot interaction," in *2023 32nd IEEE International Conference on Robot and Human Interactive Communication (RO-MAN)*. IEEE, 2023, pp. 2238–2244.
- [3] N. V. Valtakari, R. S. Hessels, D. C. Niehorster, C. Viktorsson, P. Nyström, T. Falck-Ytter, C. Kemner, and I. T. Hooge, "A field test of computer-vision-based gaze estimation in psychology," *Behavior Research Methods*, vol. 56, no. 3, pp. 1900–1915, 2024.
- [4] M. Rudling, P. Nyström, G. Bussu, S. Bölte, and T. Falck-Ytter, "Infant responses to direct gaze and associations to autism: A live eye-tracking study," *Autism*, vol. 28, no. 7, pp. 1677–1689, 2024.
- [5] J. Li, Z. Chen, Y. Zhong, H.-K. Lam, J. Han, G. Ouyang, X. Li, and H. Liu, "Appearance-based gaze estimation for asd diagnosis," *IEEE Transactions on Cybernetics*, vol. 52, no. 7, pp. 6504–6517, 2022.
- [6] J. Liu, J. Chi, W. Hu, and Z. Wang, "3d model-based gaze tracking via iris features with a single camera and a single light source," *IEEE Transactions on Human-Machine Systems*, vol. 51, no. 2, pp. 75–86, 2020.
- [7] K. Wang and Q. Ji, "Real time eye gaze tracking with 3d deformable eye-face model," in *Proceedings of the IEEE International Conference on Computer Vision*, 2017, pp. 1003–1011.
- [8] X. Cai, J. Zeng, S. Shan, and X. Chen, "Source-free adaptive gaze estimation by uncertainty reduction," in *Proceedings of the IEEE/CVF Conference on Computer Vision and Pattern Recognition*, 2023, pp. 22 035–22 045.
- [9] Y. Cheng and F. Lu, "Dvgaze: Dual-view gaze estimation," in *Proceedings of the IEEE/CVF International Conference on Computer Vision*, 2023, pp. 20 632–20 641.
- [10] T. Xu, B. Wu, R. Fan, Y. Zhou, and D. Huang, "Fr-net: a light-weight fft residual net for gaze estimation," *arXiv preprint arXiv:2305.11875*, 2023.
- [11] V. Nagpure and K. Okuma, "Searching efficient neural architecture with multi-resolution fusion transformer for appearance-based gaze estimation," in *Proceedings of the IEEE/CVF winter conference on applications of computer vision*, 2023, pp. 890–899.
- [12] F. Chollet, "Xception: Deep learning with depthwise separable convolutions," in *Proceedings of the IEEE conference on computer vision and pattern recognition*, 2017, pp. 1251–1258.
- [13] A. Howard, M. Sandler, G. Chu, L.-C. Chen, B. Chen, M. Tan, W. Wang, Y. Zhu, R. Pang, V. Vasudevan *et al.*, "Searching for mobilenetv3," in *Proceedings of the IEEE/CVF international conference on computer vision*, 2019, pp. 1314–1324.
- [14] Z. Liu, Y. Lin, Y. Cao, H. Hu, Y. Wei, Z. Zhang, S. Lin, and B. Guo, "Swin transformer: Hierarchical vision transformer using shifted windows," in *Proceedings of the IEEE/CVF international conference on computer vision*, 2021, pp. 10 012–10 022.
- [15] X. Zhang, S. Park, T. Beeler, D. Bradley, S. Tang, and O. Hilliges, "Eth-xgaze: A large scale dataset for gaze estimation under extreme head pose and gaze variation," in *Computer Vision–ECCV 2020: 16th European Conference, Glasgow, UK, August 23–28, 2020, Proceedings, Part V 16*. Springer, 2020, pp. 365–381.
- [16] P. Kellnhofer, A. Recasens, S. Stent, W. Matusik, and A. Torralba, "Gaze360: Physically unconstrained gaze estimation in the wild," in *Proceedings of the IEEE/CVF international conference on computer vision*, 2019, pp. 6912–6921.
- [17] X. Zhang, Y. Sugano, M. Fritz, and A. Bulling, "It's written all over your face: Full-face appearance-based gaze estimation," in *Proceedings of the IEEE conference on computer vision and pattern recognition workshops*, 2017, pp. 51–60.
- [18] T. Fischer, H. J. Chang, and Y. Demiris, "Rt-gene: Real-time eye gaze estimation in natural environments," in *Proceedings of the European conference on computer vision (ECCV)*, 2018, pp. 334–352.
- [19] B. Li, Y. Hu, X. Nie, C. Han, X. Jiang, T. Guo, and L. Liu, "Dropkey for vision transformer," in *Proceedings of the IEEE/CVF Conference on Computer Vision and Pattern Recognition*, 2023, pp. 22 700–22 709.
- [20] Z. Chen and B. E. Shi, "Appearance-based gaze estimation using dilated-convolutions," in *Asian Conference on Computer Vision*. Springer, 2018, pp. 309–324.
- [21] Y. Cheng and F. Lu, "Gaze estimation using transformer," in *2022 26th International Conference on Pattern Recognition (ICPR)*. IEEE, 2022, pp. 3341–3347.
- [22] J. O. Oh, H. J. Chang, and S.-I. Choi, "Self-attention with convolution and deconvolution for efficient eye gaze estimation from a full face image," in *Proceedings of the IEEE/CVF Conference on Computer Vision and Pattern Recognition*, 2022, pp. 4992–5000.
- [23] A. A. Abdelrahman, T. Hempel, A. Khalifa, A. Al-Hamadi, and L. Dinges, "L2cs-net: Fine-grained gaze estimation in unconstrained environments," in *2023 8th International Conference on Frontiers of Signal Processing (ICFSP)*. IEEE, 2023, pp. 98–102.
- [24] H. Wang, J. O. Oh, H. J. Chang, J. H. Na, M. Tae, Z. Zhang, and S.-I. Choi, "Gazecaps: Gaze estimation with self-attention-routed capsules," in *Proceedings of the IEEE/CVF conference on computer vision and pattern recognition*, 2023, pp. 2669–2677.
- [25] R. Zhao, Y. Wang, S. Luo, S. Shou, and P. Tang, "Gaze-swin: Enhancing gaze estimation with a hybrid cnn-transformer network and dropkey mechanism," *Electronics*, vol. 13, no. 2, p. 328, 2024.
- [26] S. Wang and Y. Huang, "Suppressing uncertainty in gaze estimation," in *Proceedings of the AAAI Conference on Artificial Intelligence*, vol. 38, no. 6, 2024, pp. 5581–5589.
- [27] X. Ding, X. Zhang, J. Han, and G. Ding, "Scaling up your kernels to 31x31: Revisiting large kernel design in cnns," in *Proceedings of the IEEE/CVF conference on computer vision and pattern recognition*, 2022, pp. 11 963–11 975.